Cavitating Flows of Varying Temperature Liquid Nitrogen in Converging-diverging Nozzle

Tairan Chen, Wendong Liang, Mindi Zhang, Biao Huang, Guoyu Wang*

School of Mechanical Engineering, Beijing Institute of Technology, Beijing, RP China

Abstracts

The objective of this paper is to investigate the unsteady cavitating flows of varying temperature liquid nitrogen. Liquid nitrogen cavitating flows in a converging-diverging (C-D) nozzle are carried out with the temperature range from 68 K to 86 K, the pressure in the tanks is within the range of 0.03 MPa~0.30 MPa. The experimental results show that there are two typical cavitation dynamics in varying temperature liquid nitrogen, namely classical mode and thermo-sensitive mode. As the free-stream temperature increases, the cavity area increases to its maximum around the transition temperature and then significantly decreases. Further analysis indicates that the liquid/vapor density ratio D dominates the change of the cavitation dynamics when the temperature is below the transition temperature. The cavity tends to be mushier (smaller bubbles) and longer with the increasing temperature. However, the thermodynamic effects on cavitation, which could suppress the development of the cavitating flow, dominate the change of the cavitation dynamics when the temperature is above the transition temperature. The transition temperature of cavitating flows in liquid nitrogen is between 76 K~78 K, and the transition temperature slightly increases with the increasing cavitation number.

Key words: Cavitating flows; Liquid nitrogen; Cavitation dynamics; Transition temperature

Introduction

Cavitation is a phase-change phenomenon that occurs in the liquid when the local static pressure drops below the saturated vapor pressure, this phenomenon in room temperature water is usually assumed to be an isothermal process [1,2]. However, the isothermal hypothesis is no longer valid for thermo-fluids. The temperature-dependent physical properties of thermo-fluids are thermosensitive. Furthermore, the significant temperature drop ΔT during the cavitation process changes the local physical properties, and then cavitation dynamics is affected [3,4]. Cavitation with thermodynamic effects was firstly investigated by Stahl and Stepanoff [5]. They conducted a B-factor method to estimate the thermodynamic effects during phase-change process based on a simple heat balance between these two phases. Holl et al. [6] conducted comprehensive experiments of cavitation in water and Freon 113 under different free-stream conditions with four test models. They developed a semiempirical entrainment theory to correlate the measured temperature drop ΔT. Brennen [1] developed another appropriate thermodynamic parameter named Σ by incorporating the thermodynamic effect into the Rayleigh-Plesset equation for cavitation bubble dynamics. The above parameters propose a criterion to evaluate the strength of thermodynamic effects.

To directly investigate cavitation dynamics of cavitating flows in thermo-fluids, Hord [7,8] measured the temperature and pressure data around the cavity region in liquid nitrogen and liquid hydrogen under a lot of free-stream conditions, which is the most comprehensive experimental data so far. However, it lacks of unsteady visualization and data because of the technological limitation. Recently, Franc et al. [3] investigated the

* Corresponding author, Guoyu Wang: wangguoyu@bit.edu.cn

thermodynamic effects on a cavitating inducer in R-114, they found that the development of blade cavitation was suppressed at higher reference temperature due to thermodynamic effects. Cervone et al. [9] carried out experiments in varying temperature water around a NACA 0015 hydrofoil to investigate the thermodynamic effects on cavitation dynamics. They found that the cavity length increased with the increasing free-stream temperature. Ohira et al. [10] experimentally investigated the cavitation instability of subcooled liquid nitrogen in two types of converging-diverging circular nozzle. As the temperature decreases, the cavitation mode changed from continuous mode to intermittent mode, and the transition temperature was approximately around 76 K. Kelly and Segal [11] investigated the cavitating flows of fluoroketone in a wide range of velocities, cavitation numbers, and temperatures. They pointed out the transition from classical to thermo-sensitive cavitation for fluoroketone taken place around T_∞=323 K. Zhu et al. [12] experimentally investigated the dynamic characteristics of liquid nitrogen cavitating flow through a venturi tube. The spatial changes of the temperature, pressure as well as the flow rate, together with the visual observation of unsteady cavitation behaviors were presented.

Although the cavitation dynamics in thermos-fluids have been deeply investigated in the past decades, the transition from classical to thermo-sensitive cavitation and the specific thermodynamic effects on cavitation dynamics in a wide range of temperatures are still not well understood. The objectives of this work are to present and evaluate the change of cavitation dynamics in varying temperature liquid nitrogen.

Experimental apparatus and conditions

The experimental apparatus for liquid nitrogen cavitating flows in a converging-diverging (C-D) nozzle is shown in Fig. 1(a). The apparatus essentially consisted of a run tank (capacity 40 L), the test nozzle and a catch tank (capacity 60 L), all of them are thermally protected with vacuum insulation. The temperature of liquid nitrogen is increased by increasing the pressure in both tanks by closing all the valves. And it is reduced from the atmospheric boiling point by simultaneously reducing the pressure in both tanks by using vacuum pumps. The pressure in both tanks can also be quickly increased by charging high-purity nitrogen gas. At the beginning of the experiment, the liquid nitrogen is flowed back and forth several times between these two tanks to ensure that the temperatures of the liquid nitrogen and the apparatus are steady. In the experiments, after pressurizing the liquid nitrogen in the run tank with high-purity nitrogen gas, the control valve is quickly opened to allow the liquid nitrogen to flow through the turbine flow meter and the test section to the catch tank. The test section is equipped with an assembled converging-diverging (C-D) square nozzle with a stainless steel body, Teflon bottom, and quartz glass side windows. As shown in Fig. 1(b), the test section is a C-D nozzle with an overall length of 258 mm, the inner width of 5 mm, inner heights of 20 mm on both upstream side and downstream side. The actual height of throat is 1.58 mm (the design value is 1.5 mm), which is measured by a series of needle gauges at room temperature. Considering the thermal expansion at 77 K (the thermal expansion coefficients of stainless steel and Teflon are $1.7\times10^{\wedge-5}$ (m/m K) and $8.6\times10^{\wedge-5}$ (m/m K), respectively), the change difference due to thermal expansion is 0.39 mm. And hence, the actual height of throat at 77 K is approximately 1.97 mm. The key area of the C-D nozzle is equipped with visualization windows of quartz glass with the length of 70 mm and height of 7 mm.

As previously indicated, the temperatures of the liquid nitrogen in the upstream and downstream of the C-D nozzle, the run tank and the catch tank are measured by Cernox thermometers (Lake Shore Cryotronics, Inc., accuracy ±16 mK at 77 K). The pressures in both tanks, upstream and downstream, as well as the diverging section, of the C-D nozzle are measured by absolute pressure sensors (Helm Instrument Co., Inc., range 0~0.6Mpa, accuracy ±0.1% FS). A turbine flowmeter (Hoffer flow controls, Inc., range 1.3~13.2 L/min, accuracy ±0.25%) is

fixed at the upstream of C-D nozzle, to measure the volumetric flow rate. At the same time, cavitating flows are captured for total 1 s via a high-speed video camera (Redlake Co., Inc.) with the resolution of 496×128 pixels at a frame rate of 12000 fps. The spatial resolution of the images is 0.0625 mm/pixel. To sufficiently illuminate the cavitating flow, a LED lamp (Larson Electronics LLC, 160 W-21,600 Lumens) is used and positioned at the back of text section. Experiments are carried out with varying temperature liquid nitrogen from 68 K to 86 K, the pressure in the tanks is set within the range of 0.03 MPa ~0.30 MPa. Assuming the liquid nitrogen is an incompressible fluid without phase change, throat velocity (U_{throat}) is calculated by the volumetric flow rate based on the continuity equation.

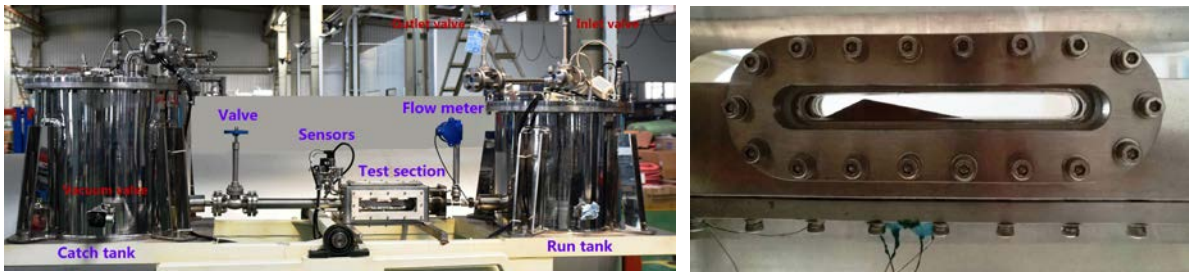

(a) Experimental apparatus (b) Test section (C-D nozzle)

Figure 1 Experimental apparatus and test section for cavitating flows of liquid nitrogen

Results and discussion

The cavitation number σ, which is defined in Eq. (1), is used to characterize the state of the cavitating flow.

$$\sigma = \frac{p_{up} - p_v(T_{throat})}{p_{up} - p_{down}} \tag{1}$$

Here, p_{up} is the upstream static pressure of the C-D nozzle, p_{down} is downstream static pressure, and p_v is the saturated vapor pressure at throat temperature T_{throat}. The average of the upstream temperature T_{up} and downstream temperature T_{down} are used to indicate the throat temperature (T_{throat}) of liquid nitrogen.

An example of typical cavitating flow observed in the experiments is presented in Fig. 2, which includes the original visualization, the schematic interpretations drawn and the processed cavity area via an in-house feature-recognition code [13]. For every moment, the original image is firstly changed into the grayscale image. Next, the grayscale value of each pixel is changed to be 255 (white) if its original grayscale value is above 100 (clean the background). And then, the wall in the image is cut by using a non-cavitation image. Finally, the cavity area is calculated by counting the numbers of the pixel whose grayscale value is not 255. The time evolution of the cavity area over a period of 1 s (12000 images) is processed for each test condition. And then, the cavity scale, the development of cavitation and the frequency analysis are quantitatively characterized.

Figure 2 Typical flow visualization and schematic interpretation of cavity area (black shadow is the cavity)

(σ=1.41, T_{throat}=73.06 K, U_{throat}≈13.8m/s)

Fig. 3(a) illustrates the relationships among time-averaged cavity area, cavitation number and temperature in the throat. The cavitation conditions are indicated by solid dots (•) and the non-cavitation conditions are indicated by stars (*). The contour is drawn by the experimental data of cavitation conditions. At any given temperature, the non-cavitation flow changes to cavitating flow as the cavitation number is reduced. The blue boundary approximately indicates the incipient cavitation number versus temperature, and the incipient cavitation number

decreases with the increasing temperature because of the increasing saturated vapor pressure. The lower red boundary indicates that the visualization window has been fully filled with cavity. It is worth noting that the cavity area increases and then decreases with the increasing temperature under the same cavitation number. The cavity area increases to its maximum value when the temperature is around 78 K. This behavior is quite different from the cavitation behaviors with strong thermodynamic effects in liquid nitrogen we used to know, while it is similar to the change of cavitation dynamics in varying temperature water and fluoroketone [4,9,11,14]. The change tendency in Fig. 3(a) is not convincing because the throat velocities of these test conditions are different. And hence, cases with similar throat velocity (U_{throat}≈13.8m/s) are selected and illustrated in Fig. 3(b). It is found the change tendency is almost the same as that in Fig. 3(a). As the temperature increases, the cavity area increases to its maximum value at the transition temperature (76 K~78 K) and then decreases under the same cavitation number. It is also found that the transition temperature slightly increases with the increasing cavitation number.

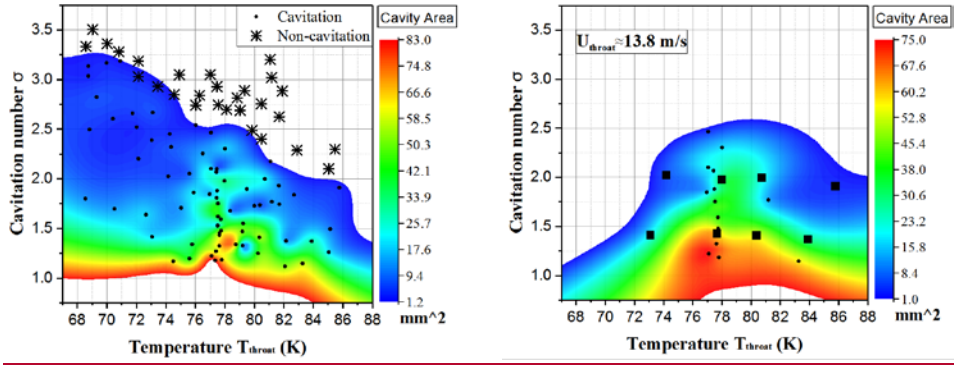

(a) All test conditions (b) Throat velocity U_{throat}≈13.8m/s

Figure 3 Distributions of time-averaged cavity area versus throat temperature and cavitation number

To further show the behavior change of cavitating flow in varying temperature liquid nitrogen. Typical of attached and shedding cavity along the diverging section for these eight cases (black square ■ in Fig. 3(b)) under the same cavitation numbers and similar throat velocity are illustrated in Fig. 4. It is shown the length of attached cavity for cavitation number σ=1.41 is approximatively 10 mm, while the length for cavitation number σ=1.98 is only approximatively 5 mm. Since the attached and shedding cavities appear as shadows, the darker is the color, the greater is the fraction of the vapor phase. It is found the liquid-vapor interface of shedding cavity is clear for T_{throat}=73.06 K and T_{throat}=74.16 K, where cavity is observed to disappear immediately after shedding. As the throat temperature increases, the shedding cavity turns to be mushier and frothier. Bubbles inside and around the shedding cavity turn to be smaller and collapse more slowly. It is because the liquid/vapor density ratio D is relatively large when the temperature is close to its triple point. Meanwhile, the local changed temperature due to thermodynamic effects is small. Assuming cavitation occurs in a finite volume, there is only one nucleation site in this finite volume, and all the liquid in the finite volume evaporates. The radius of a single spherical cavitation bubble can be conducted from the mass conservation, ($r^{\wedge}3 4\pi/3=V_v=V_l\rho_l/\rho_v=V_lD$). For cavitating flow, large density ratio D means large radius bubbles forming the cavity, and hence, the interface of the cavity is clear As the throat temperature increases, bubbles inside the cavity turns to be smaller because of the reduced density ratio D, the smaller bubbles tend to move more quickly, separate and coalesce more easily, so that the cavity turns to be mushier and frothier as observed in Fig. 4.

The increase of cavity area is because the thermodynamic effects on cavitation, which could suppress the development of cavitation, are relatively slight when the temperature is close to its triple point. Meanwhile, the smaller bubbles inside the cavity tend to collapse more slowly and move more quickly with the increasing

temperature. However, the thermodynamic effects significantly enhance with the increasing temperature. The influence of density ratio *D* is less than the thermodynamic effects when the temperature is above the transition temperature. And then, the cavity area significantly decreases with the increasing temperature. The transition means the cavitation dynamics transits from the classical mode to the thermo-sensitive mode. It is found that the transition temperature slightly increases with the increasing cavitation number in Fig. 3(b). This is because thermodynamic effects are reduced due to less mass transfer from liquid to vapor under higher cavitation number.

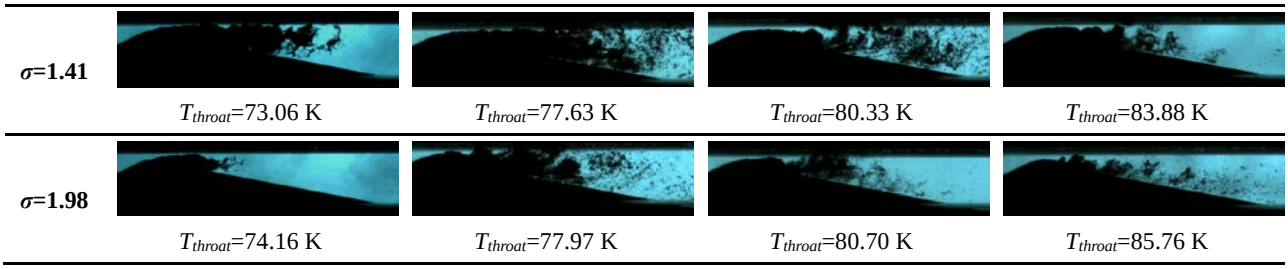

Figure 4 Cavitating flows of liquid nitrogen in converging-diverging nozzle under different flow conditions (U_{throat}≈13.8m/s)

Conclusion

Unsteady cavitating flows of liquid nitrogen under a wide range of free-stream conditions were experimentally investigated. The cavity structure, pressure and temperature, as well as the volumetric flow rate are captured by a simultaneous sampling system. The experimental results show that there are two typical cavitation dynamics in varying temperature liquid nitrogen under similar flow conditions, namely classical mode and thermo-sensitive mode. As the free-stream temperature increases, the cavity area increases to its maximum around the transition temperature and then significantly decreases. Further analysis indicates that the liquid/vapor density ratio *D* dominates the change of the cavitation dynamics when temperature is below the transition temperature. The cavity tends to be mushier (smaller bubbles) and longer with the increasing temperature. However, the thermodynamic effects on cavitation, which could suppress the development of the cavitating flow, dominate the change of the cavitation dynamics when temperature is above the transition temperature. The transition temperature of cavitating flows in liquid nitrogen is between 76 K~78 K, and the transition temperature slightly increases with the increasing cavitation number.

Acknowledgment

This work was supported by the National Natural Science Foundation of China under Grant Nos. 51479002 and 51679005. The authors also gratefully acknowledge the support by the China Scholarship Council (No. 201706030018) and Graduate Technological Innovation Project of Beijing Institute of Technology (No. 2017CX10016).

References

[1] C.E. Brennen, Cavitation and bubble dynamics, Oxford University Press, 1995.

[2] G. Wang, I. Senocak, W. Shyy, T. Ikohagi, S Cao, Dynamics of attached turbulent cavitating flows, Prog Aerosp Sci. 37 (6) (2001) 551-581.

[3] J.P. Franc, C. Rebattet, A. Coulon, An experimental investigation of thermal effects in a cavitating inducer, J. Fluids Eng. 126 (5) (2004) 716-723.

[4] T. Chen, B. Huang, G. Wang, Numerical study of cavitating flows in a wide range of water temperatures with special emphasis on two typical cavitation dynamics, Int. J. Heat Mass Tran. 101 (2016) 886-900.

[5] H.A. Stahl, A.J. Stepanoff, Thermodynamic aspects of cavitation in centrifugal pumps, J. Fluids Eng. 78 (1956) 1691-1693.

[6] J.W. Holl, M.L. Billet, D.S. Weir, Thermodynamic effects on developed cavitation, J. Fluids Eng. 97 (4) (1975) 507-513.

[7] J. Hord, Cavitation in liquid cryogens II-hydrofoils, NASA CR-2156 (1973a).
[8] J. Hord, Cavitation in liquid cryogens III-Ogives, NASA CR-2242 (1973b).
[9] A. Cervone, C. Bramanti, E. Rapposelli, L. d'Agostino, Thermal cavitation experiments on a NACA 0015 hydrofoil, J. Fluids Eng. 128 (2) (2006) 326-331.
[10] K. Ohira, T. Nakayama, T. Nagai, Cavitation flow instability of subcooled liquid nitrogen in converging–diverging nozzles, Cryogenics, 52(1) (2012) 35-44.
[11] S. Kelly, C. Segal, Characteristics of Thermal Cavitation on a Two-Dimensional Hydrofoil, J. Propul. Power 29(2) (2013) 410-416.
[12] J. Zhu, H. Xie, K. Feng, X. Zhang, M. Si, Unsteady cavitation characteristics of liquid nitrogen flows through venturi tube, Int. J. Heat Mass Tran., 112 (2017) 544-552.
[13] B. Huang, Y.L. Young, G. Wang, W. Shyy, Combined experimental and computational investigation of unsteady structure of sheet/cloud cavitation, J. Fluids Eng., 135(7) (2013) 071301.
[14] T. Chen, B. Huang, G. Wang, H. Zhang, Y. Wang, Numerical investigation of thermo-sensitive cavitating flows in a wide range of free-stream temperatures and velocities in fluoroketone, Int. J. Heat Mass Tran., 112 (2017) 125-136.